

Investigation of the electrochemical behavior of some catechols in the presence of 4,6-dimethylpyrimidine-2-thiol

Lida Fotouhi,^{a,*} Mona Khakpour,^a Davood Nematollahi,^b and Majid M. Heravi^a

^aDepartment of Chemistry, School of Science, Alzahra University, P.O.Box 1993891176, Tehran, Iran

^bDepartment of Chemistry, Faculty of Science, Bu-Ali-Sina University, P. O. Box 65174 Hamadan, Iran

E-mail: lfotouhi@alzahra.ac.ir

Abstract

The mechanism of electrochemical oxidation of catechol (**1a**), 3-methylcatechol (**1b**), 3-methoxycatechol (**1c**) and 4-methylcatechol (**1d**) in the presence of 4,6-dimethylpyrimidine-2-thiol (**3**) as a nucleophile has been studied in an aqueous solution using cyclic voltammetry and controlled potential coulometry. The results indicate that the catechol derivatives (**1a-d**) are converted to 4,5-bis (4,6-dimethylpyrimidin-2-ylthio) benzene-1,2-diol derivatives (**6a-c**) and 3,5-bis (4,6-dimethylpyrimidin-2-ylthio)benzene-1,2-diol (**6d**) through Michael addition of **3** to anodically generated o-quinones (**2a-d**). The electrosynthesis of **6(a-d)** has been successfully performed in an undivided cell in good yields and purities.

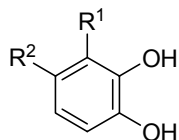
Keywords: Cyclic voltammetry, Michael addition, catechol, oxidation, 4,6-dimethylpyrimidine-2-thiol

Introduction

Catechols are well known in biological systems often as a reactive center of electron transfer in the structure of many natural compounds^{1,2} and biologically reactive molecules capable of exhibiting both anti- and pro-oxidant behavior.³ Because electrochemical oxidation very often parallels the oxidation of catechols in the mammalian central nervous system and this process occurs in the human body⁴ it was interesting to study the anodic oxidation of catechols in the presence of various nucleophiles.⁵ The quinones formed are quite reactive and can be attacked by nucleophiles such as: methanol,⁶ 4-hydroxycoumarin,⁷ 4-hydroxy-6-methyl-2-pyrone,⁸ 6-methyl-1,2,4-triazine-3-thion-5-one⁹ and so on.

On the other hand, because of the pharmacological uses of pyrimidines, the synthesis and pharmacological properties of pyrimidine,¹⁰ derivatives have been extensively investigated. In

this direction, electrochemical oxidations of catechols in the presence of barbituric acids as nucleophiles have been investigated.¹¹ In continuation of our work to synthesis of compounds with a pyrimidine moiety on the catechol ring, we have investigated the electro-oxidation of catechols in the presence of **3** as a nucleophile and described a facile one-pot electrochemical method for synthesis of some new pyrimidines derivatives.



R ¹ =H	R ² =H	1a , catechol
R ¹ =CH ₃	R ² =H	1b , 3-methylcatechol
R ¹ =OCH ₃	R ² =H	1c , 3-methoxycatechol
R ¹ =H	R ² =CH ₃	1d , 4-methylcatechol

Results and Discussion

Electro-oxidation of catechol and 3-alkyl derivatives (**1a-c**)

Cyclic voltammety of 1mM catechol (**1a**) in phosphate buffer solution (c=0.20 M, pH=7.20) shows one anodic (A₁) and corresponding cathodic peak (C₁) at 0.29 and 0.12 V, vs. Ag/AgCl due to a quasi-reversible two-electron oxidation of catechol to *o*-benzoquinone and vice versa (Fig. 1). On the other hand, the peak current ratio (I_p^{C₁}/I_p^{A₁}) of nearly unity can be considered as a criterion for the stability *o*-quinone produced at the surface of electrode under the experimental conditions. As it can be seen from Figure 1b, the cathodic counterpart of the anodic peak A₁ disappeared in the presence of **3** as a nucleophile. The positive shift of the A₁ peak in the presence of **3** that was enhanced during the repetitive recycling of potential is probably due to the formation of a thin film of product at the surface of the electrode, inhibiting to a certain extent, the performance of the electrode process. Curve b in Figure 1 shows a new anodic peak at less positive potential, 0.18 V (A₀). This new peak is related to electrooxidation of intermediate **4a** which due to the presence of an electron-donating group, is oxidized easier than starting molecule **1a**.

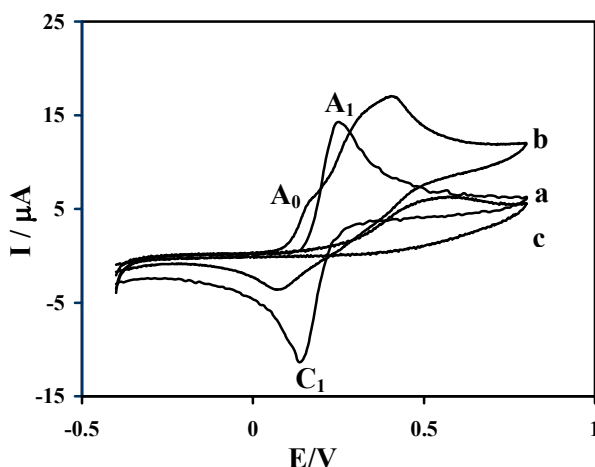


Figure 1. Cyclic voltammograms of 1 mM aqueous catechol **1a**: (a) in the absence, (b) in the presence of 1mM **3**, (c) 1mM **3** in the absence of catechol **1a** at the glassy carbon electrode in aqueous phosphate buffer ($c=0.20$ M, $\text{pH}=7.20$), scan rate: 100 mVs^{-1} .

Furthermore, it is seen that proportional to the increase in potential scan rate, the height of the C_1 peak of **1a** increases. A similar situation is observed when the **3** to **1a** concentration ratio is decreased. The increasing peak current ratio ($I_p^{C_1}/I_p^{A_1}$) and decreasing of current function ($I_p^A/\nu^{1/2}$) with increasing scan rate have been adapted as being indicative of the ECEC mechanism.

Controlled potential coulometry was performed in aqueous solution 0.10 mmol of **1a** and 0.20 mmol of **3** at 0.40 V vs. Ag/AgCl. Monitoring of the electrolysis proportional to the advancement of coulometry, anodic peak A_1 decreases and disappears when the charge consumption becomes about 4e per molecule of **1a** (Fig. 2).

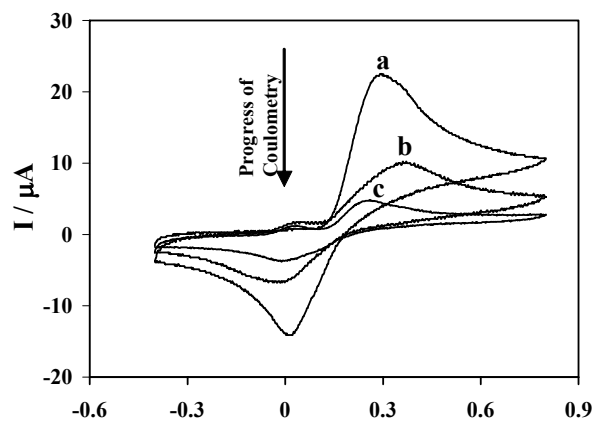


Figure 2. Cyclic voltammograms of 0.10 mmol catechol in the presence of 0.2 mmol **3**, at glassy carbon electrode during controlled potential coulometry 0.40 V vs. Ag/AgCl. (a) At beginning; (b) and (c) at the progress of coulometry. Scan rate 100 mV s^{-1} .

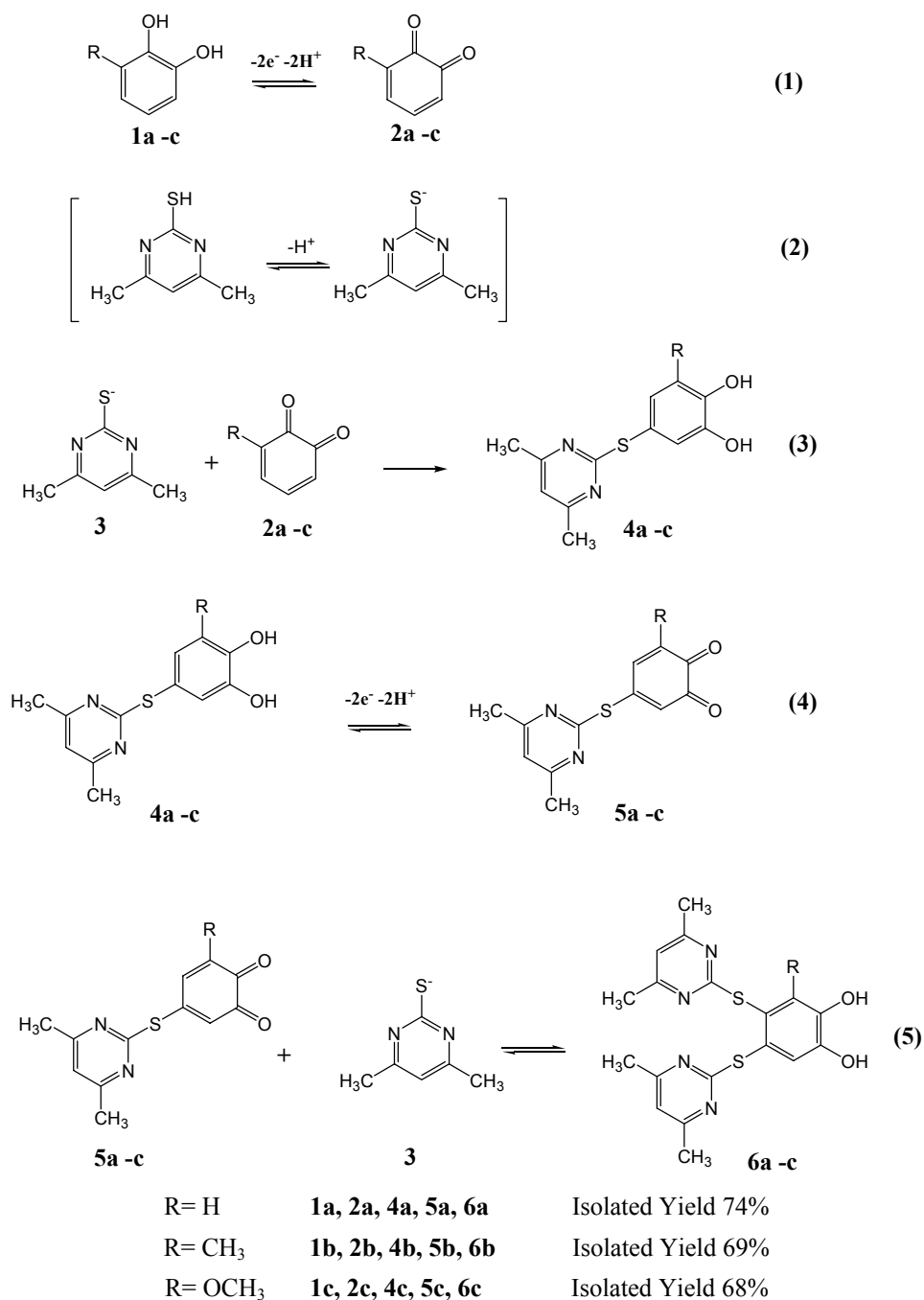
These observations allow us to propose the pathway in Scheme 1 for the electro-oxidation of **1a** in the presence of **3**. According to our results, it seems that the 1,4-Michael addition reaction of **3** to *o*-quinone (**2a**) (Eq.(3)) is faster than other secondary reactions leading to the product **4a**.

The electrochemical oxidation of this compound (**4a**) is easier than oxidation of parent starting molecule (**1a**) by virtue of the presence of an electron donating group. Then like *o*-quinone **2a**, *o*-quinone **5a** can also be attacked from the C-4 position by **3** to form final product **6a**. The overoxidation of **6a** was circumvented during the preparative reaction because of the insolubility of the product in phosphate buffer solution media.

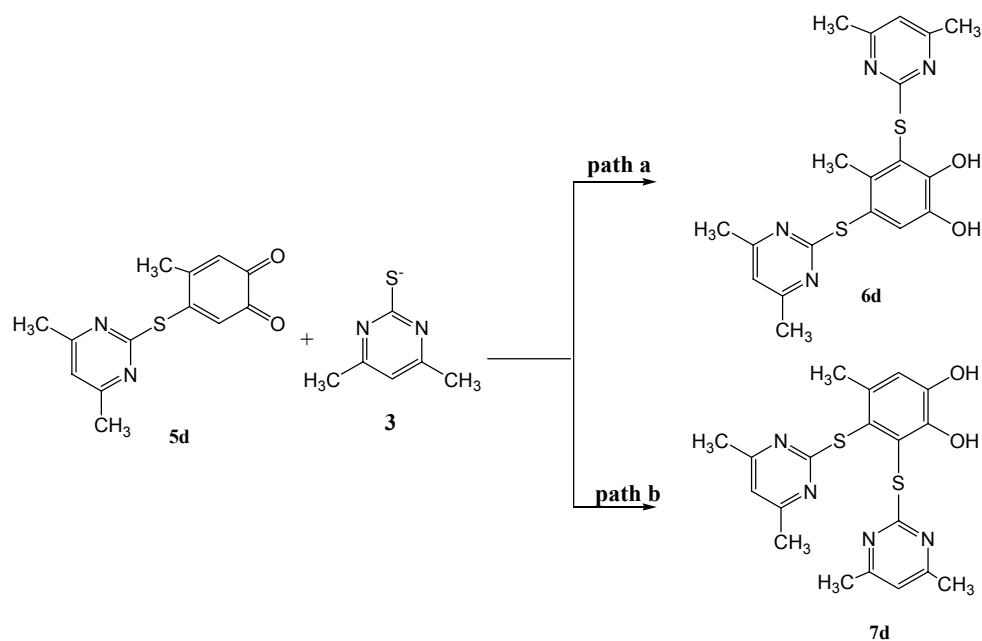
The electro-oxidation of **1b-c** in the presence of **3** as a nucleophile in buffer solution proceeds in a way similar to that of **1a**. In the all cases the presence of methyl or methoxy groups as electron-donating substituents on the molecular ring causes a diminution in activity of *o*-quinones **2b-c** as Michael acceptors toward the 1,4-addition reactions. However, the plot of peak current ratio versus scan rate confirms the reaction between *o*-quinones **2b-c** and **3**, appearing as increases in peak current ratio, I_p^{C1}/I_p^{A1} with increasing ν . According to our results, it seems that the chemical reaction between *o*-quinones **2b-c** and **3** is fast enough and leads to the formation of the products **6b-c**, respectively.

Electro-oxidation of 4-methylcatechol (**1d**)

The electro-oxidation of 4-methylcatechol (**1d**) in the presence of **3** proceeds in a similar way to that of **1a-c**. After formation of *o*-quinone **5d** via 1,4 Michael addition reaction (Eq. (3)) and oxidation (Eq. (4)), it can be attacked by the **3** from C-3 or C-6, to yield two types of products (**6d** and **7d**). The comparison of experimental and calculated ^1H NMR results of aromatic proton¹² for obtained product and suggested possible structures (**6c** and **7c**, Scheme 2) show that the *o*-benzoquinone **5d** is attacked only in the C-3 position by **3**. Thus, according to our previous results¹³ as well as the less strict effect, we think that *o*-quinone **5d** is attacked in all probability by the **3** from C-3 (path a), leading to the formation of the product **6d**.



Scheme 1

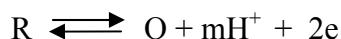


Scheme 2

The effect of pH

The influence of pH on the electrochemical behavior of catechol both in absence and presence of **3** was studied through the examining the electrode response at various pH. The position of the redox couple was found to be dependent upon pH. Cyclic voltammograms detailing the oxidation of 1mM catechol in the absence and in the presence of 1mM **3** at pH 4.00, 5.00, 6.00, 7.00 and 8.00 were compared in Figure 3. In acidic and neutral media catechols in the absence of **3** gave a well developed quasi-reversible wave (Figure 3, pH 4.00-7.00). Under these conditions, peak current ratio (I_p^{C1}/I_p^{A1}) of nearly unity can be considered as a criterion for the stability of *o*-quinone produced at the surface of the electrode under the experimental conditions. In basic solutions, the peak current ratio is less than unity and decreases with increasing pH (Figure 3, pH 8.00). These changes can be related to the coupling of the anionic or dianionic forms of catechols with *o*-quinones (dimerization reactions).¹⁴

As Figure 3 shows, the peak potentials for peaks A₁ and C₁ shifted to the negative potentials by increasing pH. This is expected because of the participation of proton in the oxidation reactions of **1a-d** to **2a-d** and **4a-d** to **5a-d**.



Where R stands for **1a**, **4a**, **1b**, **4b**, **1c**, **4c**, **1d** and **4d**; O stands for **2a**, **5a**, **2b**, **5b**, **2c**, **5c**, **2d** and **5d**; and m is the number of protons involved in the reaction.

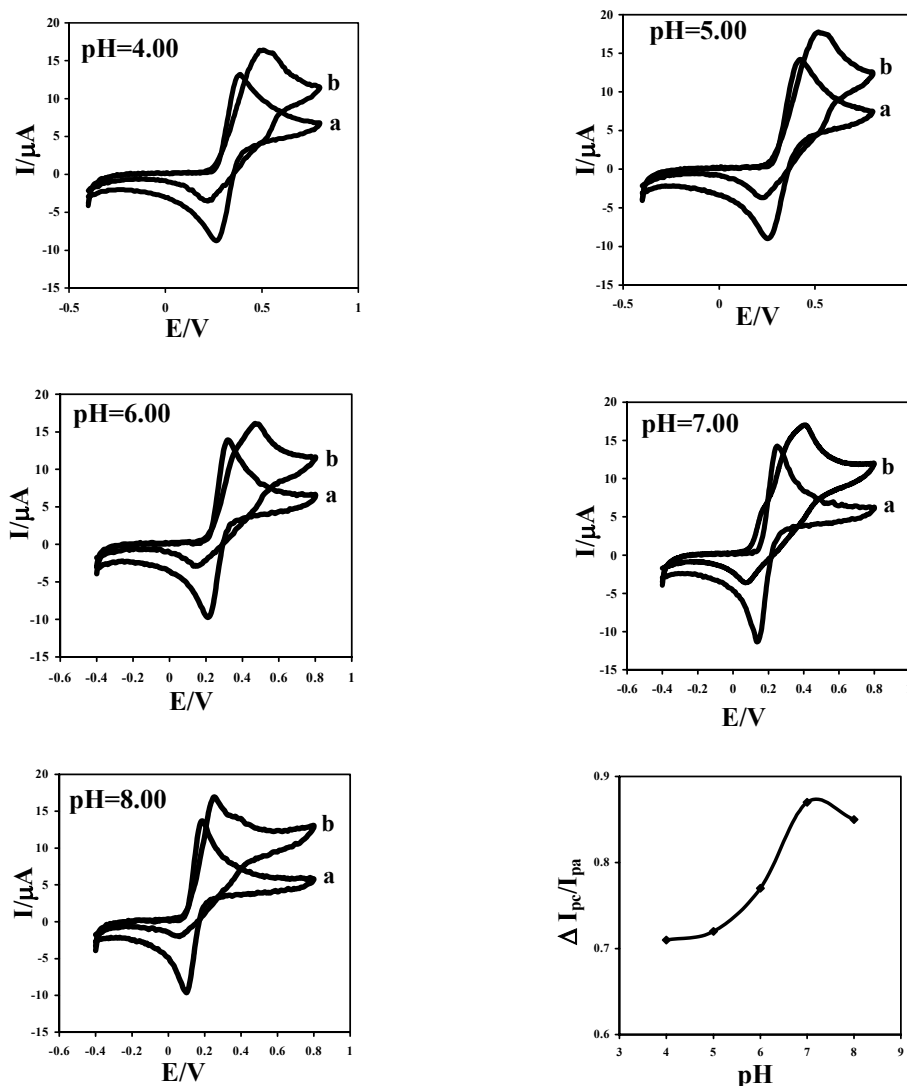


Figure 3. Cyclic voltammograms of 1mM catechol: (a) in the presence, (b) in the absence of 1mM of **3** at a glassy carbon electrode, in buffered solution (various pH). Scan rate: 100 mV s^{-1} . Analysis results: difference between peak current ratio (I_p^{C1}/I_p^{A1}) in the presence and absence of **3**.

The formal potential (E^0), which is approximated by the midpoint potential (E_{mid}) between the anodic and cathodic peaks, for this reaction scheme, the E^0 is the formal potential at pH 0.00, and R, T and F have their usual meanings. The half-wave potential ($E_{1/2}$) of catechol/*o*-benzoquinone redox couple were calculated as the average of the anodic (A_1) and cathodic (C_1) peak potentials of the cyclic voltammograms ($(E_{pa}+E_{pc})/2$) for **1a-d** and then they are plotted as a function of pH of the solution. This E^0 was shifted to negative potentials with the slope of 56 mV/pH. In all cases, the slopes are in good agreement with the theoretical slope ($2.303mRT/2F$) of 59/pH with $m=2$. Therefore, the electrochemical reaction occurring at a pH below 8.00 is a

two-electrons, two protons process. On the other hand the peak current ratio of catechol in the presence of **3** increases with decreasing pH. This can be related to protonation of the anion of **3** and its deactivation towards a Michael addition reaction, which enhanced by a decrease in pH. Because of the decrease in the rate of the polymerization reaction at pH 7.00, and an increase in the rate of the coupling reaction of **2a** and **3**, a solution containing phosphate buffer (pH 7.00, 0.20 M) has been selected as a suitable medium for electrochemical study and electrosynthesis (Fig. 3).

Experimental Section

Apparatus and Materials. Cyclic voltammetry was performed using a Metrohm model 746VA trace analyzer connected a 747 VA stand. A glassy carbon electrode (0.20 mm diameter) was used as the working electrode which was polished sequentially with alumina powder. A platinum wire and a commercial KCl Ag/AgCl electrode from Metrohm were used as the auxiliary and reference electrodes, respectively. The solutions were purged with 99.999% argon for 10 min before the start of the experiments.

Electrosynthesis was performed using a PP200 ZAHNER Elektrik potentiostat/galvanostat. The working electrode used in electrosynthesis was an assembly of four carbon rods (6 mm diameter and 4 cm length) and large platinum gauze constituted the counter electrode.

Catechols were reagent-grade from Aldrich and sodium acetate was of pro-analysis grade from E. Merck. All other chemicals were of proanalysis grade from Merck. These chemicals were used without further purification.

General Procedures. In a typical procedure, 80 ml aqueous solution containing 0.15 M sodium acetate (or phosphate buffer, C = 0.20 M, pH = 7.20) was pre-electrolyzed at 0.40 V vs. Ag/AgCl, in an undivided cell, subsequently, 1 mmol of each catechol (**1a-d**) and 4,6-dimethylpyrimidine-2-thiol (**3**) (2 mmol) were added to the cell. The electrolysis was terminated when the decay of the current became more than 95%. The process was interrupted during the electrolysis and the carbon anode was washed in acetone in order to make it reactive. At the end of electrolysis, a few drops of acetic acid were added to the solution and the cell was placed in refrigerator overnight and then the precipitate was filtrated and washed with water. All products were characterized using IR, ¹H-NMR and MS.

4,5-Bis(4,6-dimethylpyrimidin-2-ylthio)benzene-1,2-diol (6a). C₁₈H₁₈N₄O₂S₂, Mp >300 °C. IR (KBr): ν (cm⁻¹) 3383, 1584, 1487, 1343, 1260, 535. ¹H NMR (300 MHz DMSO-d₆₀, δ / ppm): 2.26 (s, 12H, methyl); 6.92 (s, 2H, catechol); 7.12 (s, 2H, pyrimidine). MS; m/e (relative intensity): 386 (30), 352 (32), 310 (15), 288 (20), 248 (65), 182 (20), 140 (56).

4,5-Bis(4,6-dimethylpyrimidin-2-ylthio)-3-methylbenzene-1,2-diol (6b). C₁₉H₂₀N₄O₂S₂, Mp >300 °C. IR (KBr): ν (cm⁻¹) =3449, 2924, 1585, 1530, 1440, 12690, 1030, 552. ¹H NMR (300

MHz DMSO- d_6 , δ / ppm) : 2.10 (s, 3H, methyl of catechol); 2.24 (s, 6H, methyl of pyrimidine); 2.26 (s, 6H, methyl of pyrimidine); 6.81 (s, 1H, catechol); 6.91 (s, 1H, aromatic proton of pyrimidine), 7.07 (s, 1H, aromatic proton of pyrimidine). MS; m/e (relative intensity): 400 (9.36), 384 (15.60); 368 (64.56); 313 (18); 293 (50); 262 (83.32); 247 (55), 229 (25); 140 (28).

4,5-Bis(4,6-dimethylpyrimidin-2-ylthio)-3-methoxybenzene-1,2-diol (6c). $C_{19}H_{20}N_4O_3S_2$, Mp >300 °C. IR (KBr): ν (cm^{-1}) = 3485, 2927, 1583, 1531, 1343, 1260, 1073, 549. 1H NMR (300 MHz DMSO- d_6 , δ / ppm) : 2.22 (s, 6H, methyl); 2.25 (s, 6H, methyl); 3.63 (s, 3H, OCH₃); 6.87 (s, 1H, catechol ring proton); 6.92 (s, 1H, aromatic proton of pyrimidine), 7.00 (s, 1H, aromatic proton of pyrimidine), 9.15 (s, 1H, OH catechol), 9.86 (s, 1H, OH catechol). MS; m/e (relative intensity): 416 (17.86), 383 (100); 367 (25); 278 (75); 188 (15); 140 (57.14).

3,5-Bis(4,6-dimethylpyrimidin-2-ylthio)-4-methoxybenzene-1,2-diol (6d). $C_{19}H_{20}N_4O_2S_2$, Mp >300 °C. IR (KBr): ν (cm^{-1}) = 3445, 1584, 1437, 1261, 1031, 554. 1H NMR (300 MHz DMSO- d_6 , δ / ppm) : 2.25 (s, 6H, methyl); 2.22 (s, 6H, methyl); 2.11 (s, 3H, methyl of catechol); 6.78 (s, 1H, catechol); 6.98 (s, 1H, aromatic proton of pyrimidine), 7.00 (s, 1H, aromatic proton of pyrimidine), 9.00 (s, 1H, OH catechol), 9.23 (s, 1H, OH catechol). MS; m/e (relative intensity): 400 (37), 368 (15); 335 (28); 262 (50); 229 (100); 140 (40).

Acknowledgements

The authors gratefully acknowledge partial financial support from the research council of Al-Zahra University.

References and Notes

1. Thomson, R. H. In *Naturally Occurring Quinones*, 3rd Edn; Chapman and Hall: London, 1987
2. Hostettmann, K., Lea I. P. In: *Biologically Active Natural Products*; Oxford University Press: Oxford, 1988
3. Chichirau, A.; Flueraru, M.; Chepelev, L. L.; Wright, J. S.; Willmore, W. G.; Durst, T.; Hussain, H. H.; Charron, M. *Free Radic. Biol. Med.* **2005**, *38*, 344.
4. Chen, S. M.; Peng, K. T. *J. Electroanal. Chem.* **2003**, *547*, 179.
5. (a) Golabi, S. M.; Nematollahi, D. *Electroanalysis* **2001**, *13*, 1008. (b) Grujic, Z.; Tabakovic, I.; Trkovic, M. *Tetrahedron Lett.* **1967**, 4823. (c) Nematollahi, D.; Forooghi, Z. *Tetrahedron* **2002**, *58*, 4949.
6. Nematollahi, D.; Golabi, S. M. *J. Electroanal. Chem.* **2000**, *481*, 20.
7. Golabi, S. M.; Nematollahi, D. *J. Electroanal. Chem.* **1997**, *420*, 127.
8. Tabakovic, I.; Grujic, Z.; Bejtovic, Z. *J. Heterocyclic Chem.* **1983**, *20*, 635.

9. (a) Fotouhi, L.; Taghavi Kiani, S.; Nematollahi, D.; Heravi, M. M. *Inter. J. Chem. Kint.* **2007**, 340. (b) Fotouhi, L.; Mosavi, M.; Heravi, M. M.; Nematollahi, D. *Tetrahedron Lett.* **2006**, 47, 8553. (c) Fotouhi, L.; Nematollahi, D.; Heravi, M. M.; Tammari, E. *Tetrahedron Lett.* **2006**, 47, 1713.
10. (a) Pani, A.; Obino, P.; Guarracine, P.; LaColla, P. *Experientia* **1994**, 50, 29. (b) Lindstad, R. I.; Mckinley-Mckee, J. S. *FEBS Lett.* **1997**, 408, 157. (c) Ramasamy, K.; Imamura, N.; Hanna, N. B.; Finch, R. A.; Avery, T. L.; Robins, R. K.; Revankar, G. R. *J. Med. Chem.* **1990**, 33, 1220.
11. (a) Abdel Azzem, M.; Zahran, M.; Hagagg, E. *Bull. Chem. Soc. Jpn.* **1994**, 67, 1390. (b) Szanto, D.; Trinidad, P.; Walsh, F. *J. Appl. Electrochem.* **1998**, 28, 251. (c) Nematollahi, D.; Goodarzi, H. *J. Electroanal. Chem.* **2001**, 510, 108. (d) Nematollahi, D.; Goodarzi, H.; Tammari, E. *J. Chem. Soc., Perkin Trans.* **2002**, 4, 829. (e) Nematollahi, D.; Hesari, M.; Davarani, S. S. H. *ARKIVOC* **2006**, 10, 129.
12. The calculated ^1H NMR results for aromatic proton of **6b** and **7b** (using *CS ChemDraw Ultra, Version 6.0, CambridgeSoft Corporation, 100 Cambridge Park Drive, Cambridge, MA 02140 USA*) shows that the aromatic proton in **6b** appears in more downfield than in **7b**.
13. Nematollahi, D.; Tammari, E. *Electrochimica Acta* **2005**, 50, 3648.
14. Rayn, M. D.; Yueh, A.; Wen-Yu, C. *J. Electrochem. Soc.* **1980**, 127, 1489.